**Proceedings of the ASME 2010 Dynamic Systems and Control Conference**
**DSCC2010**
**September 12-15, 2010, Cambridge, Massachusetts, USA**

# DSCC2010-4203

# SLIDING MODE CONTROL OF PIEZOELECTRIC VALVE REGULATED PNEUMATIC ACTUATOR FOR MRI-COMPATIBLE ROBOTIC INTERVENTION

**Yi Wang**
Mechanical Engineering
Worcester Polytechnic Institute
Worcester, MA 01609
wangy@wpi.edu

**Hao Su**
Mechanical Engineering
Worcester Polytechnic Institute
Worcester, MA 01609
haosu@wpi.edu

**Kevin Harrington**
Robotics Engineering
Worcester Polytechnic Institute
Worcester, MA 01609
harrington@wpi.edu

**Gregory S. Fischer**
Mechanical Engineering
Worcester Polytechnic Institute
Worcester, MA 01609
gfischer@wpi.edu

## ABSTRACT

*This paper presents the design of a magnetic resonance imaging (MRI) compatible pneumatic actuator regulated by piezoelectric valve for image guided robotic intervention. After comparing pneumatic, hydraulic and piezoelectric MRI compatible actuation technologies, we present a piezoelectric valve regulated pneumatic actuation system consisted of PC, custom servo board driver, piezoelectric valves, sensors and pneumatic cylinder. The system was proposed to investigate the control schemes of a modular actuator, which offers fully MRI compatible actuation; the initial goal is to control our MRI compatible prostate biopsy robot, but the controller and system architecture are suited to a wide range of image guided surgical application. We present the mathematical modeling of the pressure regulating valve with time delay and the pneumatic cylinder. Three sliding mode control schemes are proposed to compare the system performance. Preliminary simulation results are presented to validate the control algorithm.*

## INTRODUCTION

Recent years have witnessed the flourishing of MRI compatible robotics and its application in image-guided interventions and surgery. MRI provides high-fidelity soft tissue contrast and high spatial resolution. However, the high-field magnetic field limits the available technologies. There are a number of alternative MRI compatible actuation paradigms ranging from the traditional methods including hydraulic and ultrasonic piezoelectric to non-conventional actuation including electro-rheological fluids and electro-strictive polymer[1]. Although piezoelectric motor is the most prevalent actuator choice by far for its good dynamic performance, ease of control, compactness and low noise induced to the imaging process with proper shielding [2], the underlying friction driven working principle, presents challenge in design and application for force feedback due to nonlinearities, non-backdrivability and high wear. The high braking torque can be either an advantage or a detriment, with respect to a specific application [3].

Pneumatics is a preferred actuation method over hydraulics with regard to its cleanliness, ease of connectivity and ability to be operated at higher speeds. Recently, Stoianovici et al. [4] presented a new type of pneumatic motor encoded by optical sensors. Fischer, et al proposed a MRI compatible pneumatic robot for prostate intervention [5] and presented a comparative study which clearly indicated the advantage of pneumatic actuation under MRI environment [6]. Pneumatic actuation is promising to address the intrinsic compatibility issue by taking advantage of entire nonmagnetic parts and dielectric materials.

The desired position tracking accuracy of our actuator is 0.1 mm for image guided intervention [7-9]. The nonlinearity of pneumatics system presents significant challenges to accurate servo control. Also the difficulties in precise modeling and the varieties of surgical applications call for control robustness. Paul, et al. proposed a reduced order sliding mode controller (SMCr) for pneumatic actuators [10]. Acarman, et al. presented a SMCr with an observer for estimating position and

chamber pressures [11]. A SMCr was presented by Korondi, et al. that switched between two modes, namely a steep sliding line enabling rapid converge, and a shallow sliding line ensuring precise positioning [12]. Koshkouei, et al. proposed a higher order dynamic SMCr with improved system stability [13]. Nguyen, et al. presented a pulse width modulation SMCr with low-cost solenoid valves [14]. Ning, et al. showed a comparison of pneumatic system control techniques and development of SMCr [15, 16] with a steady state error (SSE) of 0.01 mm. [17] mentioned a global SMCr compensating unmodeled hysteresis of a piezo-driven stage. [18] proposed the effectiveness of a Lyapunov-based pressure observer for pneumatic systems. Dead time is often seen in pneumatic valve. Camacho, et al proposed a first-order-plus-dead-time (FOPDT) model with first order Taylor series expansion to simulate the system in [19].

The purpose of this paper is to present a pneumatic actuation system and control techniques based on novel piezoelectric pressure regulating valves consisted of a custom programmable servo board driver, a voltage to current converter, two piezoelectric pressure regulating valves and a MRI compatible pneumatic cylinder. Three sliding mode control schemes were proposed to address the system nonlinearity with particular focus on time delay issue. The key contribution of this paper is the selection and modeling of a piezoelectric pressure regulating valve leading to a simpler system model and demonstrates the simulation of tracking performance using three SMC schemes.

## II. SYSTEM ARCHITECTURE

The system consists of a PC, the servo board, the converter, two piezoelectric pressure regulating valves (Hoerbiger, model PRE-I), two pressure sensors (Omega, model PX309-100G5V), a force sensor (Futek, model LSB200), an encoder (US digital, model EM1-0-500), a MRI compatible pneumatic cylinder developed by Fischer G. [20] and a linear guide (Igus, model Drylin T). The schematic diagram of the pneumatic system integrated in MRI-guided interventions is shown in Fig. 1.

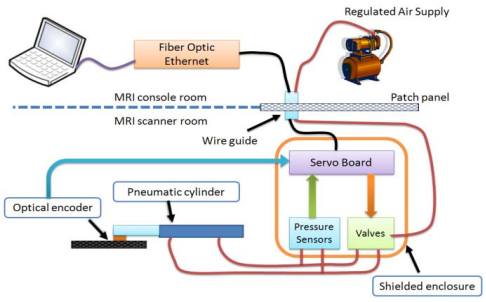


FIGURE 1. PNEUMATIC SYSTEM SCHEMATIC

Navigation software running on a PC in the console room communicates with an embedded Linux PC and the servo control board in a shielded enclosure in the scanner room via a fiber optic cable runs through the patch panel. The servo board sets control voltage of the valve based on position data as well as pressure data. The control electronics have been specially designed to operate in the scanner room without affecting MR image quality as demonstrated in [5, 6], so as to limit the length of the pneumatic transmission lines which would bring considerable delay to system performance. The laboratory testbed hardware, shown in Fig. 2, has been designed to accommodate different cylinders and payload mass. Also, it has flexibility of adding new components to the system, such as load cell, constant force spring and damper. The purpose of modular control servo board is to construct a stand-alone system that is capable of performing real-time control loops with an interface to PC program that provides set points input. It also provides on-board interfaces for quadrature optical encoder and voltage sensors. The piezoelectric valve can regulate pressure up to 689 kPa (100psi) with control input ranging from 4 mA to 20 mA. The fast response time, inherent safety of limiting pressure to a pre-determined value and MRI compatibility with proper shielding make it our first choice in valve selection. The linear optical encoder provides a resolution of 2000 counts per inch (0.01 mm precision) with quadrature mode, which is sufficient for 0.1 mm accuracy requirement. With proper choice of fasteners and shielding techniques, the encoder is also proved MRI compatible [2]. The pneumatic cylinder with 9.3 mm bore and 114 mm stroke is made of glass bore, graphite piston and brass shaft in a plastic housing.

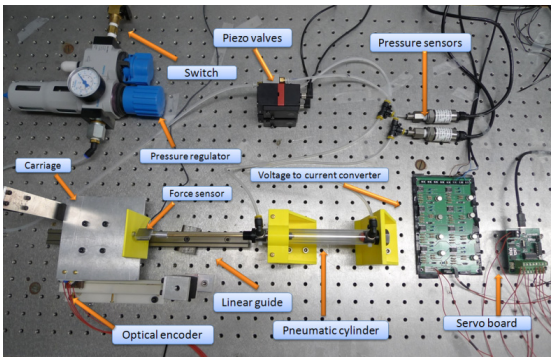


FIGURE 2. CONFIGURATION OF THE PNEUMATIC CYLINDER CONTROL TESTBED

## III. SYSTEM MODELING

### A. Pneumatic Cylinder Modeling

The schematic of the pneumatic cylinder used in the test fixture is shown in Fig. 3 [20]. Begin modeling with description

$$F_{pres} - F_{ext} = m\ddot{x} \tag{1}$$

where $F_{pres}$ is the force generated by pressure difference, $F_{ext}$ is the total external force, $m$ is the moving mass and $x$ is the position of the cylinder. We know that

$$F_{pres} = P_1 A_1 - P_2 A_2 \quad (2)$$

$$F_{ext} = F_{load} + F_{fric} \quad (3)$$

$$F_{fric} = \mu_v \dot{x} + \mu_c sign(\dot{x}) \quad (4)$$

where $P_1$ and $P_2$ are pressure of the two chambers, $A_1$ and $A_2$ are the piston areas, $F_{load}$ is the external load, $F_{fric}$ is the total friction, $\mu_v$ is the viscous friction coefficient, $\mu_c$ is the static friction coefficient. Substitute (2), (3), (4) into (1), we get

$$\ddot{x} = \frac{1}{m}[P_1 A_1 - P_2 A_2 - F_{load} - \mu_v \dot{x} - \mu_c sign(\dot{x})] \quad (5)$$

Assume no external load is applied to the cylinder. We have

$$\ddot{x} + \frac{1}{m}\mu_v \dot{x} + \frac{1}{m}\mu_c sign(\dot{x}) = \frac{1}{m}u \quad (6)$$

where $u$ is the control input and obviously $u = F_{pres}$. Setting the control input $u = kx$, where $k$ is the effective spring constant of the pneumatic cylinder holding it at set point $t = 0$, the pneumatic cylinder is a second order system.

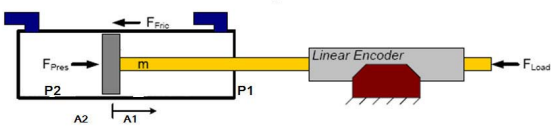


FIGURE 3. SCHEMATIC OF THE CYLINDER MODEL

### B. Piezoelectric Valve Modeling

The step responses of the valves are shown in Fig. 4. The valves exhibit dead time in step response. The FOPDT model is

$$\frac{C(s)}{R(s)} = \frac{Ke^{-t_0 s}}{\tau s + 1} \quad (7)$$

where $t_0$ is the dead time, $K$ and $\tau$ are first order system parameters. In order to simplify the model, we use a first-order expansion to approximate the exponential term

$$e^{-t_0 s} \cong \frac{1}{t_0 s + 1} \quad (8)$$

Substituting Eq. (8) into Eq. (7), we have

$$\frac{C(s)}{R(s)} \cong \frac{K}{(\tau s + 1)(t_0 s + 1)} \quad (9)$$

Write Eq. (9) in differential equation form

$$t_0 \tau \frac{d^2 C(t)}{dt^2} + (t_0 + \tau)\frac{dC(t)}{dt} + C(t) = KR(t) \quad (10)$$

The pneumatic cylinder is driven by the pressure difference of the two chambers. In practice, setting an identical pressure in both chambers in steady state and offsetting each one precisely is hard to achieve. Therefore, we seek to actuate one valve at a time and keep the other one shut. Note that $C(t)$ is the pressure of chamber, namely $P_1(t)$ or $P_2(t)$. $R(t)$ is the control signal from servo board, $U_{volt1}(t)$ or $U_{volt2}(t)$.

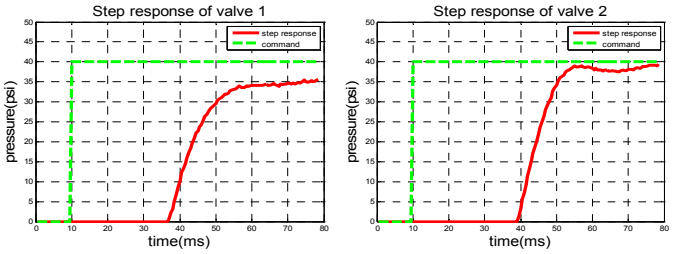


(a) (b)

FIGURE 4. STEP RESPONSES OF THE PIEZOELECTRIC PRESSURE REGULATOR VALVES

## IV. DESIGN OF CONTROL ALGORITHMS

### A. Sliding Mode Control Fundamentals

Let $X$ be denoted as the position of the pneumatic cylinder. According to Eq. 6, the state of the system is $\vec{X} = (x, \dot{x})^T$. Our goal is to ensure that the state $\vec{X}$ follows the desired state $\vec{X}_d$. The error, $\vec{E}$, is defined as

$$\vec{E} = \vec{X}_d - \vec{X} = (e, \dot{e})^T \quad (11)$$

For the cylinder plant, a suitable sliding surface function is

$$S = \lambda E + \dot{E} \quad (12)$$

where $\lambda$ represents the slope of the line $S = 0$ in the plane $(e, \dot{e})$. The solution of $S = \lambda E + \dot{E} = 0$ is

$$e(t) = e(0)\exp(-\lambda t) \quad (13)$$

In order to ensure $e(t)$ converges to zero, we need to satisfy

$$\lambda > 0 \quad (14)$$

If the states converge to the sliding surface, we derive that $\dot{S} = 0$. In order to make sure that the states always approach the sliding surface, the following condition must be met

$$S \cdot \dot{S} < 0 \quad (15)$$

Since $\dot{S}$ is the speed that sliding surface function converges to zero, fast system response with small SSE can be attained with carefully chosen $\dot{S}$ function. In the following subsections, three $\dot{S}$ functions are presented.

### B. Sliding Mode Control Scheme 1

Usually, the pneumatic cylinder control input $u$ is implemented with two elements

$$u = u_{eq} + u_s \tag{16}$$

where $u_{eq}$ is the equivalent control signal to keep the state on sliding surface once reached and $u_s$ is the switch function that compensate the state when leaving the sliding surface. To derive $u_{eq}$, substitute Eq. (6) and Eq. (11) into Eq. (12), take derivative of both sides and set left side equals to zero, we get

$$u_{eq} = m(\ddot{x}_d + \lambda_1 \dot{x}_d) + \dot{x}(\mu_v - \lambda_1 m) + \mu_c sign(\dot{x}) \tag{17}$$

The simplest form of the switching control $u_s$ is a proportional switch function

$$u_s = k_1 sign(s) \tag{18}$$

where for $s > 0$, $sign(s) = 1$, for $s < 0$, $sign(s) = -1$ and for $s = 0$, $sign(s) = 0$. However $sign(s)$ may bring chattering due to discontinuity. Replacing it by a saturation function

$$u_s = k_1 sat(s / d_1) \tag{19}$$

where $k > 0$ and for $|s| < d_1$, $u_s = k_s(s / d_1)$ and for $|s| \geq d_1$, the function becomes $u_s = k_1 sign(s / d_1)$. The control parameters $d_1$, $k_1$ and $\lambda_1$ will be manually tuned.

### C. Sliding Mode Control Scheme 2

Choose the $\dot{S}$ function to be

$$\dot{S} = -k_2 |s|^a sat(\frac{s}{d_2}) \tag{20}$$

where $k_2 > 0$ and $a > 0$. We know that

$$\dot{S} = \lambda_2 \dot{E} + \ddot{E} = \lambda_2(\dot{x}_d - \dot{x}) + (\ddot{x}_d - \ddot{x}) \tag{21}$$

We know from Eq. 6 that

$$\ddot{x} = -\frac{\mu_v \dot{x}}{m} - \frac{1}{m}\mu_c sign(\dot{x}) + \frac{u}{m} \tag{22}$$

Substitute Eq. 22, Eq. 20 into Eq. 21, we can get a function of control signal

$$u = m[\ddot{x}_d + \lambda_2 \dot{x}_d + \lambda_2 \dot{x} + k_2 |s|^a sat(\frac{s}{d_2})] + \mu_v \dot{x} + \mu_c sign(\dot{x}) \tag{23}$$

where the control parameters $a$, $d_2$, $k_2$ and $\lambda_2$ will be manually tuned.

### D. Sliding Mode Control Scheme 3

Assume we choose $\dot{S}$ function to be

$$\dot{s} = -k_3 s \tag{24}$$

where $k_3 > 0$. The solution is

$$s = s(0)e^{-k_3 t} \tag{25}$$

indicating that the sliding surface function will exponentially converge to the sliding surface. This control scheme offers a quick response when far from the sliding surface. Once the system is in the vicinity of the sliding surface, converging speed decreases to a small amount such that desired response is not attained. In order to improve the system performance, we can add a switching ramp function. Then $\dot{S}$ function is

$$\dot{s} = -k_3 s - \zeta sat(\frac{s}{d_3}) \tag{26}$$

where $\zeta > 0$ [21]. Similarly, substitute Eq. 22 and Eq. 26 into Eq. 21, we can derive the control signal

$$u = m[\ddot{x}_d + \lambda_3 \dot{x}_d - \lambda_3 \dot{x} + k_3 s + \zeta sat(\frac{s}{d_3})] + \mu_v \dot{x} + \mu_c sign(\dot{x}) \tag{28}$$

where the control parameters $\zeta$, $d_3$, $k_3$ and $\lambda_3$ will be manually tuned.

## V. SIMULATION AND RESULTS

The simulation of the system model was implemented in Matlab. The system initial state and reference input was defined before the simulation. Two inputs were selected as reference for tracking: Sine wave function $x = 0.03\sin(0.8\pi t)$ with initial position error of 0.01 m; Step function $x = 0.06(t)$. The sine wave with frequency of 0.4 Hz is selected since the speed of motion is appropriate for use in many robotic interventions. In order to evaluate the system response to a set position, step function is utilized to evaluate the time when the position tracking error is less than 0.1 mm. Then we ran the SMCr along with pneumatic cylinder to derive the control input of the pneumatic cylinder, namely $F_{pres}(t)$. With $F_{pres}(t)$, the control input of the valve $U_{volt}(t)$ was obtained by Eq. 10. The control voltage which drives the piezo valve and pneumatic

cylinder position with respect to the reference input were printed out for comparison. Table 1 shows the identified mass of the system and the manually tuned SMCr parameters. Note that $m_{\text{mod}}$ is the modified mass of the system assuming extra weights are attached to the system. The simulated tracking and control signal of the valves are shown in Fig. 5. For robustness test, we change the mass of the system $m_{\text{mod}}$ and compare the results. Noted that all control signals add 2 V offset.

TABLE 1: SIMULATION PARAMETERS OF THE SYSTEM

| **Parameter** | | | | | |
|---|---|---|---|---|---|
| $m$ | 0.3kg | $m_{\text{mod}}$ | 0.5kg | $\zeta$ | 2.2 |
| $\mu_c$ | 0.285 | $\lambda_1$ | 100 | $k_1$ | 2 |
| $d_1$ | 0.05 | $\lambda_2$ | 50 | $k_2$ | 3 |
| $d_2$ | 0.001 | $a$ | 0.1 | $\lambda_3$ | 50 |
| $k_3$ | 2.8 | $d_3$ | 0.005 | | |

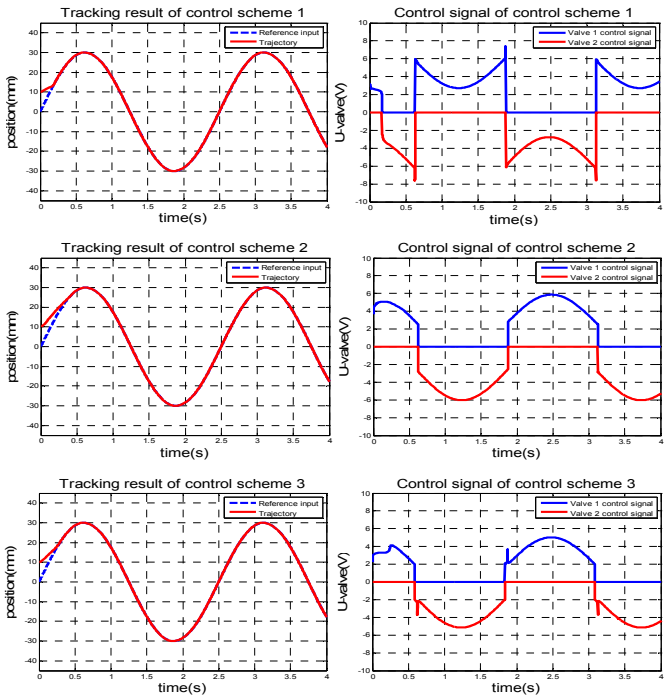


(a) TRACKING RESULT OF SINE FUNCTION AND CONTROL SIGNAL

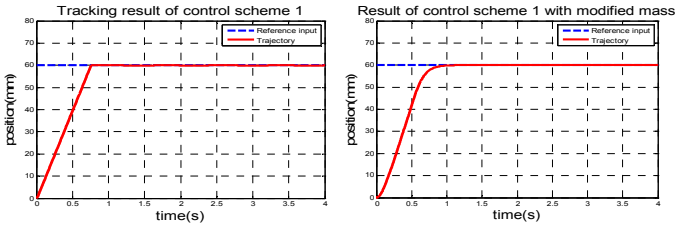


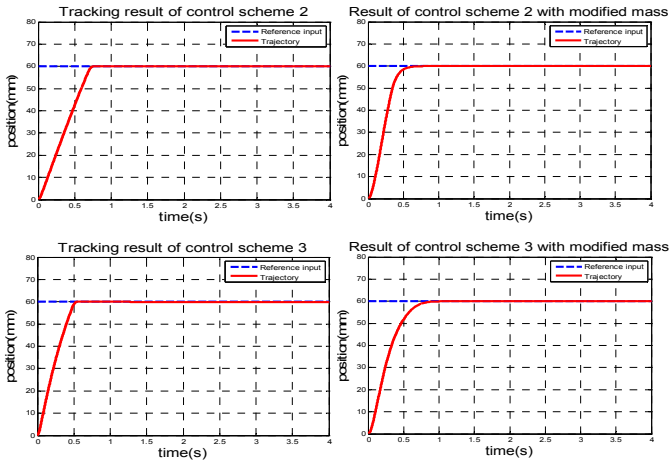


(b) STEP FUNTION ROBUSTNESS TEST WITH $m$ and $m_{\text{mod}}$

FIGURE 5. MATLAB SIMULATION RESULTS COMPARING SMC SCHEMES FOR BOTH SINE AND STEP INPUTS

All three algorithms attained the desired accuracy 0.1 mm. When tracking the sine function, the SSEs of Scheme 1, 2 and 3 are 0.092 mm, 0.058 mm and 0.079 mm. The time when cylinder achieves 0.1 mm position tracking error is 0.22 s, 0.40 s and 0.31 s respectively. In terms of tracking the step function, the time is 0.77 s, 0.75 s and 0.54s for $m$ and 0.98 s, 0.72 s and 0.95 s for $m_{\text{mod}}$. As for the control signal, Scheme 1 and Scheme 3 contain spikes which make the valve hard to follow. In terms of tracking speed, the performance of Scheme 1 and Scheme 3 is remarkable when tracking sine function and step function respectively. The performance of Scheme 2 is better than Scheme 1 and Scheme 3 with respect to position tracking accuracy, smooth signal and robustness. Therefore, Scheme 2 is the most suitable control algorithm.

## VI. CONCLUSION

Pneumatics is a preferable method for MRI compatible actuation. A test system has been built to evaluate control algorithms. Due to fast response and MRI compatibility, a novel piezoelectric pressure regulating valve was utilized. An approximated system model was established with regards to dead time induced by valve response and model uncertainty. SMC was adopted for testing tracking accuracy and response time. Three SMC schemes were proposed and the performances were evaluated by Matlab simulation. Considering position tracking accuracy, converging time, amount of chattering in control signal and robustness, Scheme 2 is regarded as the best algorithm. Despite the assumption that only one valve operates at a time, we noticed that the operation time of both valves might overlap for less than 3 ms. The influence is yet to be determined. The future work is to carry out comparison of the algorithms on the physical system to validate the simulation results. The calculation complexity of the three schemes varies. Therefore, it could potentially slow down the control loop

when running on a microcontroller and affect controller hardware choice. Last but not the least, the piezoelectric model is based on the instantaneous system state, suggesting a prior knowledge of the reference input function so as to ensure performance; this might not be very exact.

## ACKNOWLEDGMENTS

We gratefully acknowledge the support from the Congressionally Directed Medical Research Programs Prostate Cancer Research Program New Investigator Award W81XWH-09-1-0191 and Worcester Polytechnic Institute internal funds.

## REFERENCES

[1] N. V. Tsekos, A. Khanicheh, E. Christoforou, and C. Mavroidis, 2007. "Magnetic resonance - Compatible robotic and mechatronics systems for image-guided interventions and rehabilitation: A review study". *Annual Review of Biomedical Engineering*, 9, April, pp. 351-387.

[2] Y. Wang, G. Cole, H. Su, J. Pilitsis, and G. Fischer, 2009. "MRI Compatibility Evaluation of a Piezoelectric Actuator System for a Neural Interventional Robot". Proc. of IEEE Engineering in Medicine and Biology Society, MN.

[3] F. Carpi, A. Khanicheh, C. Mavroidis, and D. De Rossi, 2008. "MRI Compatibility of Silicone-Made Contractile Dielectric Elastomer Actuators". *IEEE/ASME Trans. Mechatronics*, 13(3), pp. 370-374.

[4] D. Stoianovici, A. Patriciu, D. Petrisor and L. Kavoussi, 2007. "A new type of motor: pneumatic step motor". *IEEE/ASME Trans. Mechatronics*,12, pp. 98-106.

[5] G. S. Fischer, I. Iordachita, C. Csoma, J. Tokuda, S. P. DiMaio, C. M. Tempany, N. Hata, and G. Fichtinger, 2008. "MRI-Compatible Pneumatic Robot for Transperineal Prostate Needle Placement". *IEEE/ASME Trans. Mechatronics*, 13(3), pp. 295-305.

[6] G. Fischer, A. Krieger, I. Iordachita, C. Csoma, L. Whitcomb, and G. Fichtinger, 2008. "MRI Compatibility of Robot Actuation Techniques – A Comparative Study". Proc. Medical Image Computing and Computer-Assisted Intervention, pp. 509-517.

[7] H. Su, W. Shang, G. Cole, K. Harrington, and G. Fischer, 2010. "Haptic System Design for MRI-Guided Needle Based Prostate Brachytherapy". Haptics Symposium.

[8] H. Su, K. Harrington, G. Cole, W. Lu, and G. S. Fischer, 2010. "Piezoelectrically Actuated Needle Steering System for MRI-Guided Transperineal Prostate Biopsy and Brachytherapy". Proc. IEEE Int. Conf. on Intelligent Robots and Systems (Under Review).

[9] H. Su and G. Fischer, 2009. "A 3-Axis Optical Force/Torque Sensor for Prostate Needle Placement in Magnetic Resonance Imaging Environments". Proc. IEEE Int. Conf. on Tech. for Practical Robot Applications.

[10] A. Paul, J. Mishra, and M. Radke, 1994. "Reduced order sliding mode control for pneumatic actuator". *Trans. on Contr. Systems Technology*, 2(3), pp. 271-276.

[11] T. Acarman, C. Hatipoglu, and U. Ozguner, 2001. "A robust nonlinear controller design for a pneumatic actuator". Proc. Amer. Contr. Conf., pp. 4490-4495.

[12] P. Korondi and J. Gyeviki, 2006. "Robust Position Control for a Pneumatic Cylinder". Proc. of Power Electronics and Motion Contr. Conf., pp. 513-518.

[13] A. Koshkouei, K. Burnham, and A. Zinober, 2005. "Dynamic sliding mode control design". Proc. of IEE Contr. Theory and Applications, pp. 392-396.

[14] T. Nguyen, J. Leavitt, F. Jabbari, and J. E. Bobrow, 2007. "Accurate Sliding-Mode Control of Pneumatic Systems Using Low-Cost Solenoid Valves". *IEEE/ASME Trans. Mechatronics*, 12(2), pp. 216-219.

[15] G. M. Bone and N. Shu, 2007. "Experimental Comparison of Position Tracking Control Algorithms for Pneumatic Cylinder Actuators". *IEEE/ASME Trans. Mechatronics*, 12(5), pp. 557-561.

[16] N. Shu and G. M. Bone, 2005. "Experimental comparison of two pneumatic servo position control algorithms". Proc. Int. Conf. on Mechatronics and Automation, pp. 37-42.

[17] Q. Xu and Y. Li, 2009. "Global sliding mode-based tracking control of a piezo-driven XY micropositioning stage with unmodeled hysteresis". Proc. of IEEE/RSJ Int. Conf. on Intelligent Robots and Systems, pp. 755-760.

[18] N. Gulati and E. J. Barth, 2009. "A Globally Stable, Load-Independent Pressure Observer for the Servo Control of Pneumatic Actuators". *IEEE/ASME Trans. Mechatronics*, 14(3), pp. 295-306.

[19] O. Camacho and C. Smith, 2000. "Sliding mode control: an approach to regulate nonlinear chemical processes". *ISA Trans.*, 39(2), pp. 205-218.

[20] G. Fischer, 2008, "Enabling technologies for MRI guided interventional procedures". Ph.D. thesis, Johns Hopkins University, Baltimore, MD.

[21] J. Kun, Z. Jinggang, and C. Zhimei, 2002. "A new approach for the sliding mode control based on fuzzy reaching law". Proc. of Intelligent Contr. and Automation, Vol. 1, pp. 656-660.